Journal of Solid State Chemistry 182 (2009) 2912–2917

Contents lists available at ScienceDirect

Journal of Solid State Chemistry

journal homepage: www.elsevier.com/locate/jssc

One-pot, high-yield synthesis of titanate nanotube bundles decorated by Pd (Au) clusters for stable electrooxidation of methanol

Xiudong Xue [a], Li Gu [b], Xuebo Cao [a,*], Yingying Song [a], Lianwen Zhu [a], Peng Chen [a]

[a] Key Lab of Organic Synthesis of Jiangsu Province and Department of Chemistry, Soochow University, Suzhou, Jiangsu 215123, PR China
[b] College of Biology and Chemical Engineering, Jiaxing University, Jiaxing, Zhejiang 314001, PR China

ARTICLE INFO

Article history:
Received 1 May 2009
Received in revised form
30 July 2009
Accepted 1 August 2009
Available online 8 August 2009

Keywords:
Hydrothermal synthesis
Nanotubes
Cyclic voltammetry
Electrochemical properties

ABSTRACT

Titanate nanotube bundles assembled by several simple nanotubes were synthesized through a simple reaction between TiO_2 crystallites and highly concentrated NaOH in the presence of Au or Pd sols. Due to the unique scrolling growth mechanism of titanate nanotubes (TNTs), Au or Pd clusters were encapsulated *in situ* by TNTs, and titanate/Au and titanate/Pd nanotube bundles were formed. In comparison with carbon nanotubes (CNTs) or active carbon that was widely used as carriers to support metal clusters, TNTs bundles can immobilize the metal clusters tightly and overcome the shortcoming of exfoliation of metal clusters from the carriers. The as-prepared titanate/metal hybrids possess mesoporosity and high surface area. The electrochemical oxidation of methanol demonstrates that titanate/Pd hybrids exhibit high electrocatalytic activity and excellent stability, and hence they should be ideal catalyst candidates in direct methanol fuel cells (DMFCs).

1. Introduction

Noble metal nanoclusters supported by porous carriers are important functional materials in catalysis [1] and nanoelectronics [2]. Especially, the electrocatalysis of them toward the oxidation of methanol is subjected to intense investigation due to its possible application in direct methanol fuel cells (DMFCs) which can provide green power source for portable electronic devices and electric vehicles [3,4]. Carbon nanotubes (CNTs) are usually the preferred carriers of noble metal nanoclusters because of their large surface area, good electrical conductivity, rapid mass transport arising from the anisotropic morphology, and tunable diameter, which make the metal-CNTs hybrids possess a higher electrochemical activity than those supported by the commonly used carbon black [5–7]. Generally, CNTs supported metal clusters were fabricated through a two-step strategy: CNTs were firstly grown in a vapor process and next metal clusters were reduced *in situ* on the surface of the nanotubes. Since the metal clusters were only bound onto CNTs by a weak adsorption, they would be very easily dropped from CNTs under operating conditions, which will not only cause the loss of the costly noble metal but also bring about the decrease of the catalytic activity of the metal-CNTs hybrids as well as the decrease of the oxidation current density of methanol if the metal-CNTs are used as the catalysts of DMFCs. However, the ability to provide stable current output is one of the primary aims in DMFCs. Consequently, it is essential to optimize the catalysts by developing alternative tubular carriers that can immobilize noble metal clusters tightly and utilize the costly noble metal more efficiently.

Layer-structured inorganic compounds are known to have the special property to grow into tubular nanostructures under certain conditions, of which alkaline titanates are representative samples. Titanate nanotubes (TNTs) can be easily synthesized on a large scale through a simple, low-temperature hydrothermal reaction between TiO_2 crystallites and highly concentrated NaOH [8–11], not requiring any catalysts or additives. The growth mechanism of TNTs can be described as the delamination of TiO_2 crystallites into two dimensional (2D) lamellar titanate intermediates and the subsequent curl of the nanosheet into nanotubes (Fig. 1) [8–14]. It suggests that, if TNTs are synthesized in the coexistence of metal clusters, the curl of the lamellar intermediates will result in the efficient encapsulation of metal clusters by TNTs (Scheme 1), which will result in the immobilization of metal clusters securely. Moreover, although metal clusters are located inside the TNTs, it does not obstruct the contact of methanol with metal clusters and the occurrence of catalytic reactions because TNTs are mesoporous, well permeable, and exchangeable [15–18]. Consequently, it is rational to expect that TNTs with a lower production cost should be ideal candidate to replace CNTs as the carrier for the *in-situ* immobilization of metal clusters [19,20].

Building from these ideas, herein we reacted TiO_2 crystallites with 10 M NaOH hydrothermally at 160 °C in the presence of palladium (Pd) or gold (Au) sols. TNTs bundles filled with Pd or Au

* Corresponding author. Fax: +86 512 65880089.
E-mail address: xbcao@suda.edu.cn (X. Cao).

0022-4596/$ - see front matter © 2009 Elsevier Inc. All rights reserved.
doi:10.1016/j.jssc.2009.08.001

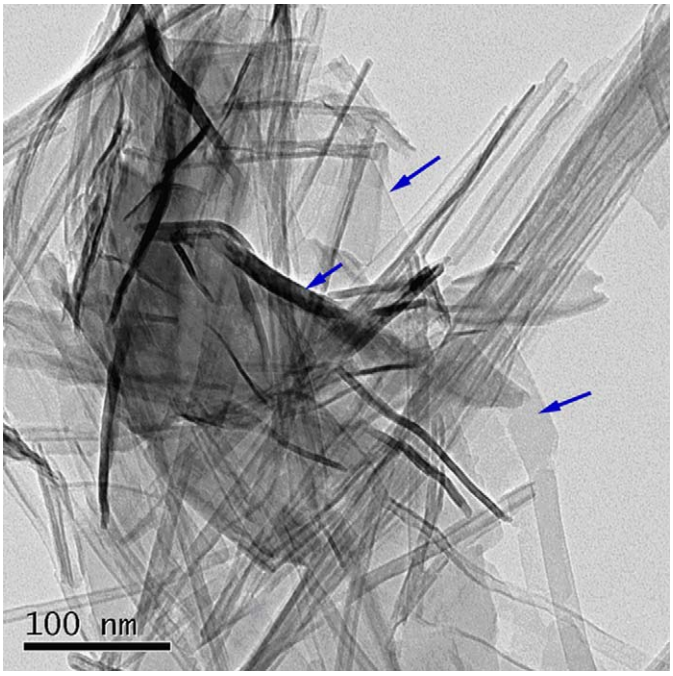

Fig. 1. TEM image shows the transformation of nanosheet intermediates into tubular structures. The nanosheets were indicated with arrows.

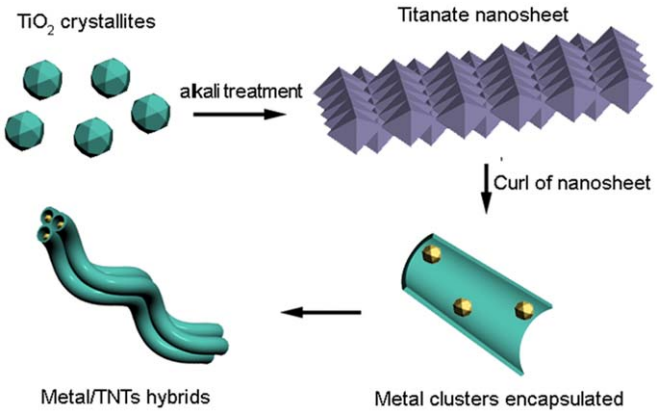

Scheme 1. Diagrammatical description of the strategy for the preparation of titanate–metal hybrids. Metal clusters are encapsulated by TNTs.

clusters were successfully synthesized. Although TNTs and TiO_2-based nanotubes have been investigated intensely since the first report by Hoyer [21], such a distinct rope morphology assembled by several simple tubular structures is rare. More importantly, the as-prepared titanate/Pd hybrids were found to exhibit obvious catalytic activity and excellent stability toward the electrooxidation of methanol.

2. Experimental

Materials: Tetrakis hydroxymethyl phosphonium chloride (THPC) was purchased from Alfa Aesar. Other reagents were purchased from Shanghai Chemical Co. All reagents were used as received.

Preparation of pure titanate and titanate–metal hybrids: For the preparation of titanate-Au and titanate-Pd hybrids, 0.1 g of TiO_2 powders was firstly dispersed into 26 mL NaOH (10 M) by ultrasound. Next, about 4.9 mg of Au (Prepared by reducing 50 mL of 25 mM $HAuCl_4$ with THPC) or 15.9 mg of Pd (Prepared by reducing 30 mL of 5 mM $PdCl_2$ with fresh $NaBH_4$ aqueous solution) were added into the dispersion under vigorous agitation. Then, the mixture was transferred into a 30 mL Teflon-lined autoclave and heated at 160 °C for three days. After cooled down to ambient temperature, titanate–metal hybrids were separated from the solution, ultrasonically washed repetitively with distilled water till pH value of the solution is neutral, and dried at vacuum at 40 °C. The preparation condition of pure titanate was the same as that of the hybrids except that there were no Pd or Au nanoparticles in the system.

Characterizations: X-ray diffraction (XRD) patterns were collected on an X'Pert PRO SUPER rA rotation anode X-ray diffractometer with Ni-filtered Cu$K\alpha$ radiation ($\lambda = 1.5418$ Å). Field-emitting scanning electron microscopy (FESEM) images were taken by a Hitachi S-4700 electron microscope (FESEM). Transmission electron microscopy (TEM) images were taken by a FEI Tecnai G20 electron microscope. High-resolution TEM (HRTEM) image was taken with a JEOL-2010 electron microscope. Energy dispersive X-ray spectrometry (EDS) analysis was performed on the spectrometer attached on Hitachi S-4700 electron microscope. The nitrogen adsorption–desorption isotherms and BET surface area were measured on a Micromeritics ASAP 2020 instrument.

Electrochemical measurements were carried out at 25 °C in a standard three-electrode cell connected to a CHI 660C electrochemical workstation (Chenhua Co., Shanghai). Pt and saturated calomel electrode (SCE) were used as the counter and reference electrode, respectively. The work electrode was prepared by casting the as-prepared titanate/Pd hybrids, titanate/Au hybrids, or pure TNTs (~0.8 mg) in 5 wt% Nafion to a glass carbon (GC) electrode with a diameter of 2 mm and allowed to dry at atmosphere. Before use, GC and Pt electrodes were carefully polished. Cyclic voltammetry (CV) was investigated between −0.8 and 0.2 V (vs. SCE) at a scan rate of 50 mV/s in the solution of 1.0 M KOH and 1.0 M CH_3OH aqueous solution. Before recording the final voltammogram, the electrode was cycled for several runs.

3. Results and discussion

Titanate/Pd hybrids and titanate/Au hybrids synthesized from the reaction between TiO_2 crystallites and highly concentrated NaOH were firstly checked by XRD technique. Shown in Fig. 2a and b were the corresponding XRD patterns of them. For the sake of comparison, XRD pattern of pure titanate was also included (Fig. 2c). A broad peak around $2\theta = 9.6°$ appears in all the three XRD patterns of Fig. 2, which is the characteristic interlayer diffraction of titanate [8–14,22,23]. Diffraction peaks corresponding to TiO_2 crystallites were not found, and hence it demonstrates that alkali treatment has completely transformed TiO_2 into monoclinic $A_2Ti_nO_{2n+1}\cdot H_2O$, where A represents Na and/or H [24]. Besides those assigned to titanate, diffraction peaks of Pd(111), Pd(200), and Pd(220) were detected in Fig. 2a and the diffraction peak of Au(200) was detected Fig. 2b. Considering that the as-prepared hybrids had been ultrasonically washed repetitively, Au and Pd clusters uncombined by titanate had been removed as much as possible. Consequently, Au and Pd detected by XRD should be those encapsulated inside the titanates. In addition, a peak centered at 28.3° is observed in XRD patterns of titanate/Au and titanate/Pd hybrids while it is absent in that of pure titanate. Generally, the increase of the intensity ratio of peak (310) to peak (110) indicates that parts of Na atoms in the titanate have been replaced by H atoms [23–26]. It is worthwhile to mention that the replacement of Na by H was not caused by the acid washing because our products were

washed only with distilled water till the pH value of the solution was neutral. Consequently, the structural difference between pure titanate and those in the hybrids was correlated with Au and Pd sols introduced into the system during the synthesis of the hybrids.

Fig. 3 shows EDS characterizations of the titanate/Pd hybrids and titanate/Au hybrids. As consistent with the results of XRD, EDS spectra also confirmed the existence of Pd (Fig. 3a) and Au (Fig. 3b), where the signals of Si arise from silicon wafer for supporting the samples. The weight fraction of Au and Pd in the hybrids is 2.76% and 6.21%, respectively. According to it, it can be inferred that the final products contain about 4.65 mg of Au and 14.31 mg of Pd, which are very close to the quantity of Pd and Au feed into the reaction system initially. That is, metal clusters in the reaction system were almost completely encapsulated by the titanate carriers.

Fig. 4 displays FESEM and TEM images of the as-prepared hybrids. Interestingly, both of the titanate/Au hybrids (parts a, b of Fig. 4) and titanate/Pd hybrids (parts c, d of Fig. 4) were composed of nanotube bundles structures on a large scale, very analogous to CNTs bundles in shape [27–29]. TEM images revealed that the titanate/Au tube bundles (Fig. 4e) was constructed by five to ten close-packed tubes and titanate/Pd tube bundles (Fig. 4f) was constructed by more tubes, and so that, titanate/Pd tube bundles are looked densely than titanate/Au tube bundles. Owing to the encapsulation of Pd and Au clusters, the interiors of the tube bundles were found to be filled with numerous small particles. For clarity, the titanate/Pd tube bundles were also observed under HRTEM, and the inset in Fig. 4f was the typical HRTEM image, which clearly revealed the presence of irregular Pd crystallites. The lattice spacing in these crystallites is about 0.23 nm, close to the *d*-spacing of (111) planes of face-centered cubic Pd (0.225 nm).

The transversal sizes of titanate/Au tube bundles and titanate/Pd tube bundles are about 70 and 100 nm, respectively. But their length cannot be exactly measured because the nanotube bundles are curly (the tube bundles are at least as long as 5 μm). In a word, the characterizations of TEM and FESEM confirmed that the strategy proposed in Scheme 1 is feasible. In addition, although there exist several previous reports on studying the supports of noble metal with TNTs [19,20,30,31], they are all prepared by the wet impregnation technique, which cannot ensure the formation of metal clusters in the interiors of TNTs. On the contrary, the strategy presented herein allows the accurate encapsulation of metal clusters by TNTs.

It is worth noting that the distinct tube bundles morphology of titanate in the hybrids is largely different from that of pure ones and is very rare in previous reports. Usually, pure titanate, obtained under experimental conditions same as the preparation of the hybrids, only presents a simple tubular structure, such as the representative sample shown in Fig. 5. For the purpose of the application of TNTs in the field of carriers, nanotube bundles should be superior to simple nanotubes because of their better strength and toughness.

The growth mechanism of the TNTs bundles is believed to be analogous to that of CNTs bundles. As we know, individual CNTs can be assembled into macroscopic bundles via van der Waals interactions [27–29]. Herein, the forces to direct the formation of TNTs bundles are hydrogen bonds. As revealed by XRD (Fig. 2), titanate in the titanate/Au and titanate/Pd hybrids has a high H/Na ratio. Due to the rich protons within nanosheet intermediates and the resulting hydrogen bonds, strong interactions should exist among the nanosheet intermediates and drive the nanosheets to be adjoined. Next, the scrolling of these adjoining nanosheets leads to the formation of TNTs bundles. Whereas the chemical composition of pure titanate is mainly $Na_2Ti_nO_{2n+1}$, and the hydrogen bonds are absent among the intermediates. Therefore, the final product for pure titanate was only composed of individual nanotubes.

The as-prepared pure TNTs and the TNTs bundles were characterized further by nitrogen isothermal adsorption/desorption at 77 K, and the recording isotherms were shown in Fig. 6a. The adsorption–desorption isotherms of the TNTs bundles and pure TNTs are both type IV and the hyteresis loops can be classified into type H3 in IUPAC classification, which is consistent

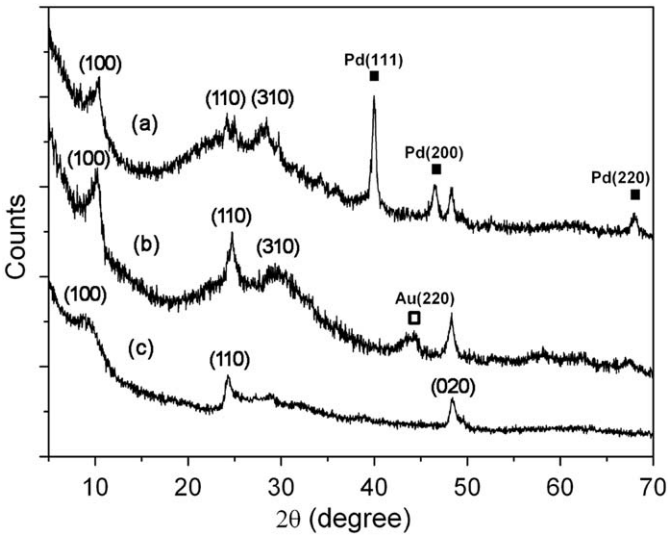

Fig. 2. XRD patterns of titanate/Pd hybrids (a), titanate/Au hybrids (b), and pure titanate (c).

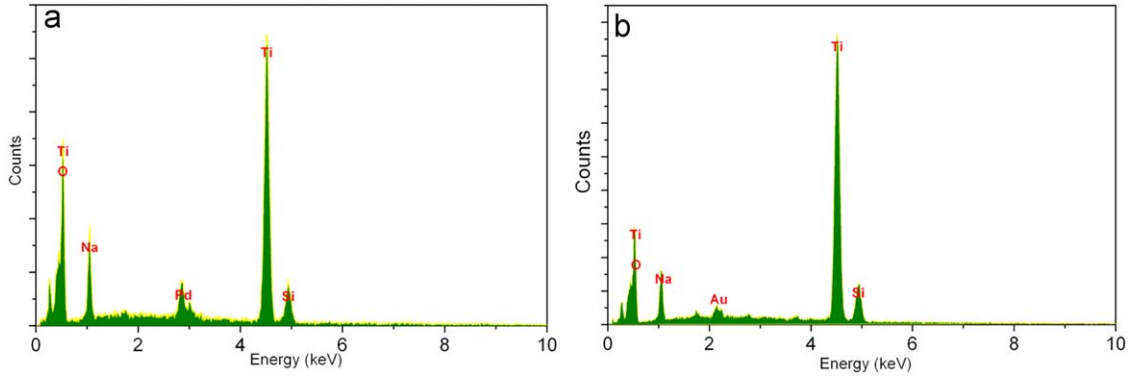

Fig. 3. EDS spectra of the hybrids: (a) titanate-Pd, (b) titanate-Au. The signals of Si arise from Si substrate of supporting the samples.

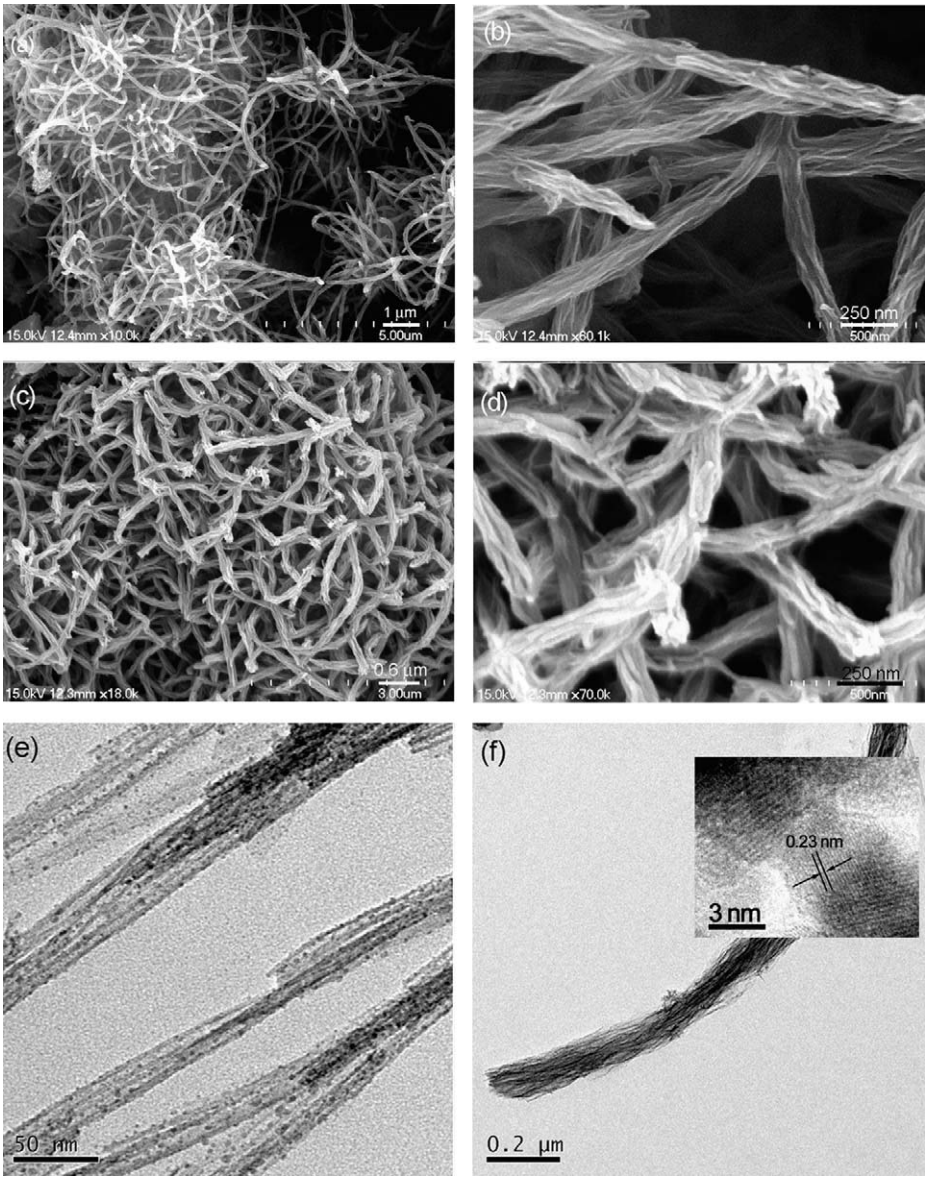

Fig. 4. (a, b) FESEM images of titanate/Au hybrids. (c, d) FESEM images of titanate/Pd hybrids. (e) TEM image of titanate/Au hybrids. (f) TEM image of titanate/Pd hybrids, where the inset is HRTEM image of Pd nanoparticles encapsulated by the nanotube bundles.

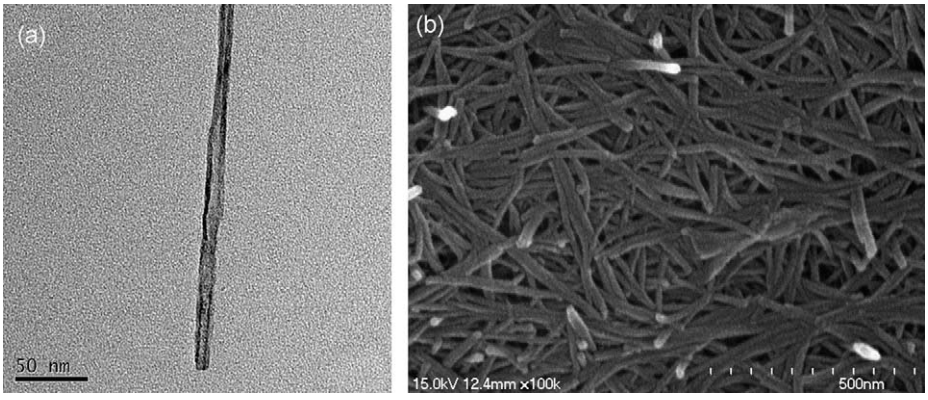

Fig. 5. Representative TEM image (a) and FESEM image (b) of pure titanates. The product presents a simple tubular structure.

with previous reports on TNTs-based materials [10,23]. These features demonstrate that the products are mesoporous and slit-shaped pores are probably formed. The BET surface area of pure TNTs, titanate/Au tube bundles, and titanate/Pd tube bundles were 258.7, 173.1, and 237.6 m^2/g, respectively. The value of the surface area of pure TNTs is identical with the previous reports

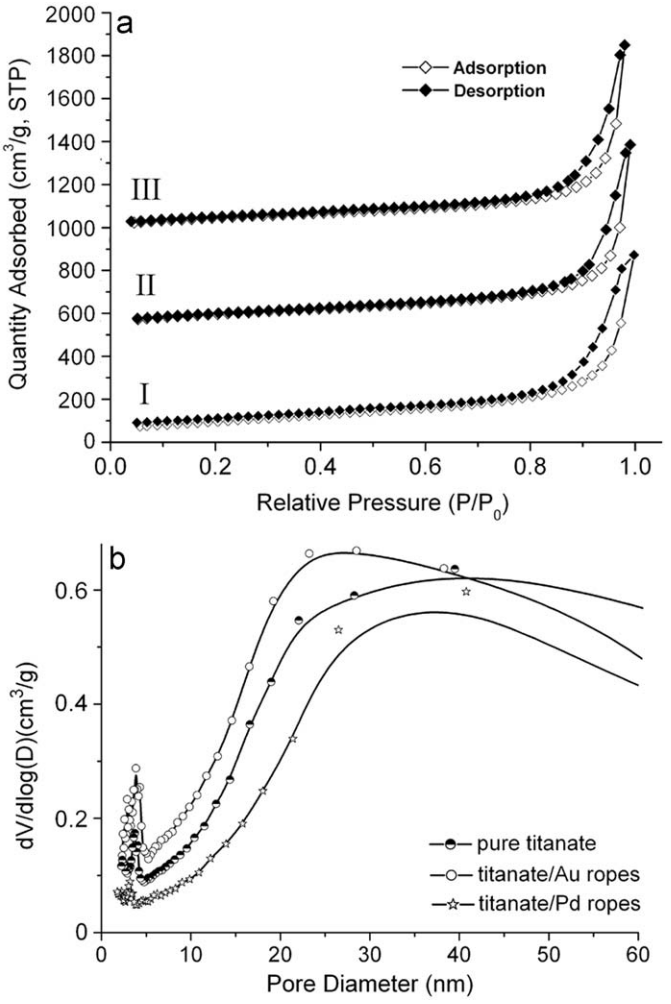

Fig. 6. (a) N_2 adsorption/desorption isotherms of pure TNTs and the hybrids. (I): Pure TNTs. (II): Titanate/Pd hybrids. (III): Titanate/Au hybrids. (b) Pore size distribution curves of pure TNTs and the two hybrids.

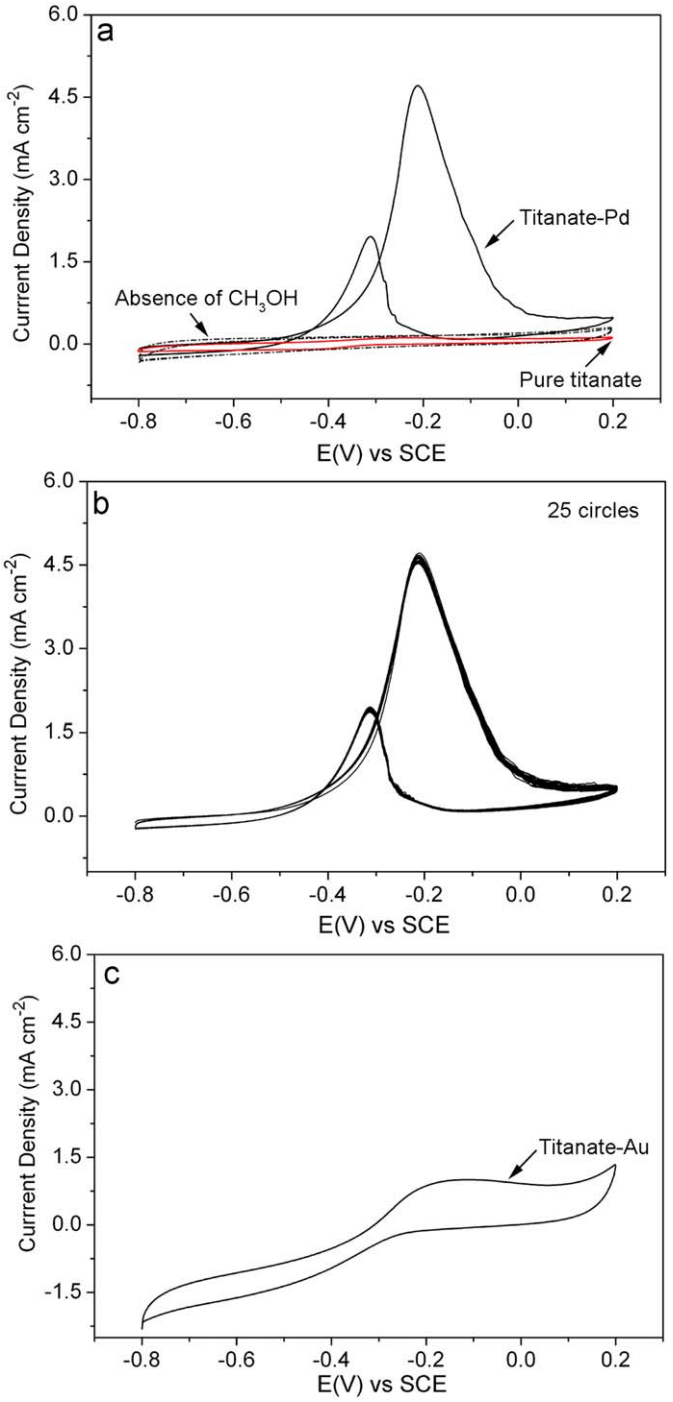

Fig. 7. (a) Black solid line: CV curve of titanate/Pd hybrids in 1.0 M KOH and 1.0 M CH_3OH; red line: CV curve of pure TNTs in 1.0 M KOH and 1.0 M CH_3OH; dash line: CV curve of titanate/Pd hybrids in 1.0 M KOH solution. (b) CV curves of titanate/Pd hybrids with 25 cycles in 1.0 M KOH and 1.0 M CH_3OH. (c) CV curve of titanate/Au hybrids in 1.0 M KOH and 1.0 M CH_3OH. All the scan rates during the measurements were 50 mV/s. (For interpretation of the references to the color in this figure legend, the reader is referred to the web version of this article.)

[10,23], whereas the smaller surface area of titanate/Au and titanate/Pd tube bundles relative to that of pure TNTs is because their interiors were filled by metal clusters. Fig. 6b shows the pore size analysis from desorption branch data, based on the Barrett–Joyner–Halenda (BJH) method, which clearly demonstrated that both pure TNTs and the hybrids possessed two kinds of mesopores. The smaller pores (~3.8 nm) are equal to the inner diameter of the nanotubes, while another pore size distribution positioned at 20–40 nm is correlated to the stacks of the tubes or the tube bundles. In a word, like pure TNTs, titanate/Au and titanate/Pd hybrids also possess rich mesopores and large surface area, which will become preferable properties if the hybrids are applied in the field of catalysis.

The electrochemical oxidation of 1.0 M CH_3OH in 1.0 M KOH at 25 °C was used to test the catalytic activity of the as-prepared titanate/Pd and titanate/Au hybrids. Black solid line in Fig. 7a corresponds to cyclic voltammetry (CV) curve using titanate/Pd hybrid as the anodic catalysts. Two oxidation peaks centered at −0.22 and −0.31 V (vs SCE) are observed, and such CV features are in agreement with those reported in the literature [32,33]. The current peak at −0.22 V (current density: 4.75 mA/cm^2) is produced due to the oxidation of freshly chemisorbed methanol, while the peak at −0.31 V is primarily associated with the removal of carbonaceous species not completely oxidized in the forward scan [34]. At $E<-0.4$ V, the curve of the forward sweep and the backward sweep almost overlaps. In the study on electrochemical oxidation of small organic molecules, this kind of CV characteristic indicates that the self-poisoning reaction is not significant [35,36].

For comparison, CV curve (dash line) in the 1.0 M KOH solution free of CH_3OH and CV curve (red line) measured on the electrode of pure TNTs are also included in Fig. 7a, which confirm that the measured current originates from electrocatalytic oxidation of

methanol. In addition, Pd-based electrodes in the alkaline media usually characterize strong anodic and cathodic peaks in the potential range of −0.8 to 0.2 V (vs SCE), owing to the oxidation of Pd and the reduction of the oxides [37,38]. However, herein the curve is rather flat, suggesting that Pd nanoclusters in TNTs bundles have a strong ability of anti-oxidation.

Fig. 7b shows CV curves with 25 cycles using titanate/Pd hybrids as the anodic catalysts. After 25 cycles, the oxidation peak current density was 4.63 mA/cm^2. It only decreases by 2.6% by comparison with the initial current density of 4.75 mA/cm^2, which demonstrates that the titanate/Pd hybrids electrode was not deactivated and possesses an extremely high stability. For the catalyst of noble metal supported on carbon, the oxidation current was usually decreased sharply after multiple scans, possibly owing to the exfoliation or poisoning of metal clusters. For instance, the current of methanol oxidization catalyzed by Pd supported on carbon was decreased from the initial 0.12 to 0.09 A (decrease by 25%) after 10 circles [39]. Consequently, herein the titanate/Pd hybrids show their merit of stability toward the electrocatalytic oxidation of methanol, which is a desired property in DMFC.

Fig. 7c shows CV curve of methanol oxidation reaction on the electrode of titanate/Au hybrids; the measurement conditions were the same as that on the electrode of titanate/Pd hybrids. It was also characterized by two well de-fined anodic current peaks, consistent with the previous report [40]. The maximum oxidation current density was about 0.96 mA/cm^2 (at −0.16 V), which is only one fifth of that catalyzed by titanate/Pd hybrids. But this value is still higher than the maximum oxidation current density of 0.11 mA/cm^2 measured on the electrode made up of pure gold nanoparticles [40]. In addition, titanate/Au hybrids electrode could also possess a good stability after multiple cycles (the results were not shown). That is, both the results of electrochemical oxidation of methanol on the electrodes made up of titanate/Au and titanate/Pd hybrids demonstrate that TNTs bundles are ideal carriers to support nanoparticles of noble metal.

4. Conclusions

In conclusion, taking advantage of the unique scrolling mechanism of TNTs, we have fabricated mesoporous TNTs bundles as carriers to immobilize Pd and Au clusters tightly, which could overcome the shortcoming of exfoliation of costly noble metal in traditional catalysts. The present strategy may also be extended to the preparation of other TNTs-based hybrids that encapsulate magnetic or semiconducting nanoclusters. The electrocatalytic oxidation of methanol demonstrates that titanate/Pd hybrids have high catalytic activity and good stability. Consequently, they should be ideal candidates as the catalysts in DMFC.

Acknowledgments

Financial supports from the key lab of organic synthesis of Jiangsu Province (PR China), "Qin-Lan" Project of Jiangsu Province, Program of Innovative Research Team of Suzhou University, and National Natural Science Foundation of China (Grant no. 20601020) were gratefully acknowledged.

References

[1] X.B. Cao, L. Gu, L.J. Zhuge, W.J. Gao, S.F. Wu, Adv. Funct. Mater. 16 (2006) 896.
[2] B.H. Morrow, A. Striolo, J. Phys. Chem. C 111 (2007) 17905.
[3] B.C.H. Steele, A. Heinzel, Nature 414 (2001) 345.
[4] S.Q. Song, P. Tsiakaras, Appl. Catal. B 63 (2006) 187.
[5] H. Tang, J.H. Chen, Z.P. Huang, D.Z. Wang, Z.F. Ren, L.H. Nie, Y.F. Kuang, S.Z. Yao, Carbon 42 (2004) 191.
[6] Y. Lin, X. Cui, C. Yen, C.M. Wai, J. Phys. Chem. B 109 (2005) 14410.
[7] A. Kongkanand, K. Vinodgopal, S. Kuwabata, P.V. Kamat, J. Phys. Chem. B 110 (2006) 16185.
[8] T. Kasuga, M. Hiramatsu, A. Hoson, T. Sekino, K. Niihara, Langmuir 14 (1998) 3160.
[9] Q. Chen, W. Zhou, G. Du, L.M. Peng, Adv. Mater. 14 (2002) 1208.
[10] C.C. Tsai, H. Teng, Chem. Mater. 16 (2004) 4352.
[11] D. Wu, J. Liu, X.D. Zhao, A.D. Li, Y.F. Chen, N.B. Ming, Chem. Mater. 18 (2006) 47.
[12] Y.Q. Wang, G.Q. Hu, X.F. Duan, H.L. Sun, Q.K. Xue, Chem. Phys. Lett. 365 (2002) 427.
[13] R. Ma, Y. Bando, T. Sasaki, J. Phys. Chem. B 108 (2004) 2115.
[14] C.C. Tsai, H. Teng, Langmuir 24 (2008) 3434.
[15] S. Uchida, Y. Yamamoto, Y. Fujishiro, A. Watanabe, O. Ito, T. Sato, J. Chem. Soc. Faraday Trans. 93 (1997) 3229.
[16] T. Sasaki, F. Kooli, M. Iida, Y. Michiue, S. Takenouchi, Y. Yajima, F. Izumi, B.C. Chakounakos, M. Watanabe, Chem. Mater. 10 (1998) 4123.
[17] D.J.D. Corcoran, D.P. Tunstall, J.T.S. Irvine, Solid State Ionics 136 (2000) 297.
[18] J.H. Choy, H.C. Lee, H. Jung, S.J. Huang, J. Mater. Chem. 11 (2001) 2232.
[19] M. Wang, D.J. Guo, H.L. Li, J. Solid State Chem. 178 (2005) 1996.
[20] J.M. Macak, P.J. Barczuk, H. Tsuchiya, M.Z. Nowakowska, A. Ghicov, M. Chojak, S. Bauer, S. Virtanen, P.J. Kulesza, P. Schmuki, Electrochem. Commun. 7 (2005) 1417.
[21] P. Hoyer, Langmuir 12 (1996) 1411.
[22] G.H. Du, Q. Chen, R.C. Che, Z.Y. Yuan, L.M. Peng, Appl. Phys. Lett. 79 (2001) 3702.
[23] T. Gao, H. Fjellvåg, P. Norby, Inorg. Chem. 48 (2009) 1423.
[24] J.N. Nian, H. Teng, J. Phys. Chem. B 110 (2006) 4193.
[25] J. Yang, Z. Jin, X. Wang, W. Li, J. Zhang, S. Zhang, X. Guo, Z. Zhang, J. Chem. Soc. Dalton Trans. (2003) 3898.
[26] C.C. Tsai, H. Teng, Chem. Mater. 18 (2006) 367.
[27] B. Vigolo, A. Penicaud, C. Coulon, C. Sauder, R. Pailler, C. Journet, Science 290 (2000) 1331.
[28] M.L. Terranova, S. Orlanducci, E. Fazi, V. Sessa, S. Piccirillo, M. Rossi, D. Manno, A. Serra, Chem. Phys. Lett. 381 (2003) 86.
[29] K.M. Liewa, C.H. Wong, M.J. Tan, Appl. Phys. Lett. 87 (2005) 1901.
[30] D.V. Bavykin, A.A. Lapkin, P.K. Plucinski, L. Torrente-Murciano, J.M. Friedrich, F.C. Walsh, Top. Catal. 39 (2006) 151.
[31] J.H. Jiang, Q.M. Gao, Z. Chen, J. Mol. Catal. A 280 (2008) 233.
[32] C.W. Xu, Z.Q. Tian, P.K. Shen, S.P. Jiang, Electrochim. Acta 53 (2008) 2610.
[33] W. Pan, X.K. Zhang, H.Y. Ma, J.T. Zhang, J. Phys. Chem. C 112 (2008) 2456.
[34] J.C. Huang, Z.L. Liu, C.B. He, L.M. Gan, J. Phys. Chem. B 109 (2005) 16644.
[35] R. Parsons, T. Vandernoot, J. Electroanal. Chem. 257 (1988) 9.
[36] S. Ha, R. Larsen, Y. Zhu, R.I. Masel, Fuel Cells 4 (2004) 337.
[37] C. Xu, L. Cheng, P. Shen, Y. Liu, Electrochem. Commun. 9 (2007) 997.
[38] R.N. Singh, A. Singh, Anindita, Int. J. Hydrogen Energy 34 (2009) 2052.
[39] M.L. Wang, W.W. Liu, C.D. Huang, Int. J. Hydrogen Energy 34 (2009) 2758.
[40] J. Hernández, J. Solla-Gullón, E. Herrero, A. Aldaz, J.M. Feliu, Electrochim. Acta 52 (2006) 1662.